치의학박사학위논문

Filling Quality of MTA Canal Obturation in Type Ⅲ Root Canal with Isthmus

Isthmus를 갖는 제 3형 근관에서 MTA를 이용한 근관 충전의 질적 평가

2016년 2월

서울대학교 대학원

치의과학과 치과보존학 전공

오 소 람

-ABSTRACT-

Filling Quality of MTA Canal Obturation in Type Ⅲ Root Canal with Isthmus

So-Ram Oh

Program in Conservative Dentistry,

Department of Dental Science

The Graduate School

Seoul National University

(Directed by Professor Kee-Yeon Kum)

Objectives

The objective of this study was to compare the filling quality of mineral trioxide aggregate (MTA) canal obturation with lateral compaction (LC) and continuous wave of condensation (CW) in type III mesial root canals with isthmuses of the mandibular first molars using micro-computed tomography (micro-CT). The null hypothesis was that there is no significant difference in filling quality among the three obturation techniques in the main root canals and the isthmus.

Materials and Methods

The mesial roots of 60 extracted human mandibular first molars with type III canal configuration by Weine that had an interconnecting isthmus were prepared to an apical size of #40. The specimens were allocated into three groups of 20 roots for obturation by either LC or CW using a gutta-percha and AH Plus sealer, or by MTA canal obturation with OrthoMTA (MTA). The obturated roots were scanned by micro-CT (Skyscan 1172). The filled volume ratio (%) in the main canal or in the isthmus at the apical third was calculated using CTAn software. The filled volume ratio was defined as the ratio of the sum of the obturated gutta-percha and sealer volume or MTA to the main canal or isthmus volume. Data were statistically analyzed using the Kruskal-Wallis test or Mann-Whitney U test applying a significance level of 0.05.

Results

Reconstructive micro-CT images demonstrated that the LC group had lower filling densities in the isthmus than either CW or MTA. Unfilled radiolucent voids were shown in two samples in the MTA group. The filled volume ratio was not significantly different among the three groups for the main canals ($p > 0.05$). In the isthmus, the filled volume ratio for LC was lower than in

CW and MTA ($p < 0.05$). The volume ratio of the gutta-percha for LC was significantly lower in the isthmus than that of CW, whereas the volume ratio of the sealer was significantly greater ($p < 0.05$).

Conclusions

MTA canal obturation showed comparable filling quality to LC or CW techniques in the main canal or isthmus.

Key Words: MTA canal obturation, Filled volume ratio, Isthmus, Micro-computed tomography, Mandibular first molar, Type III canal

Student number: 2011-30664

I. Introduction

The main purpose of root canal obturation is to obtain a three-dimensional seal of the entire root canal system that prevents communication between the root canal and periapical tissue (1). However, it is difficult to achieve this goal because of the intricate anatomical structures such as the isthmus, fin, and loops in the root canal system. Root canal isthmus, which is a thin communication between two or more canals within the same root (2), is reported to have an incidence of 50 to 85% at the apical 5 mm of the mesial roots of the mandibular molars as assessed by micro-computed tomography (micro-CT) (3, 4).

The isthmus is inaccessible to instruments and harbors pulp tissue and microbes after root canal treatment (5). In a previous study, inadequately cleaned and unfilled isthmus was observed when an endoscope was used to examine the resected root-end following root canal treatment (6). Multispecies biofilm was also observed in the isthmus by transmission electron microscope in a case of failed retreatment of a mandibular molar (7).

Most root canal obturation techniques employ a core material that is most commonly gutta-percha and a sealer (1). Lateral compaction (LC) is the standard procedure by which other obturation techniques are evaluated. However, it is time-

consuming and lacks homogeneity and surface adaptation (8). Previous studies have demonstrated that LC is inadequate for filling canal irregularities (9). Therefore, heated gutta-percha techniques were developed to better replicate irregular root canal anatomy (1). Schilder demonstrated that a warm vertical condensation technique provided homogenous, dimensionally stable filling (1). The continuous wave of condensation (CW) technique, developed by Buchanan, is a variation of the warm vertical condensation technique (10). However, an electric heat carrier or thermoplastic injection of the gutta-percha increased the temperature of the outer root surface. The root surface temperature was elevated by more than 10℃ in mandibular incisors by the Touch'n Heat (11) or System B electric heat carrier (12). Destruction of the periapical periodontal ligament was caused by thermoplastic gutta-percha injection with Obtura (13).

Root canal sealers are used to seal the space between gutta-percha and the canal wall, since gutta-percha does not adhere to dentin. However, most root canal sealers undergo dimensional changes after root canal obturation that compromises their seal (14). Therefore, MTA-based root canal sealers were recently developed because of their biocompatibility, dimensional stability, and sealing ability (15).

MTA has excellent sealing ability and enhanced biocompatibility (16). It was originally used as a root-end filling material in surgical endodontics for its excellent sealing ability (17). A previous study reported that an interfacial layer composed of calcium and phosphate forms at the MTA-dentin interface in the presence of phosphate-buffered saline (18). This characteristic structure could contribute to its sealing capacity when used as a canal filling material. Nonetheless, MTA has not been used as a routine canal filling material because of the micro- and macro-porosities of the mixture during hydration (19, 20), its difficulty in handling, associated tooth discoloration, and irretrievability (21, 22).

MTA canal obturation has been used in many clinical cases and has shown favorable outcomes as a canal obturation technique (23). One previous study demonstrated that orthograde ProRoot MTA obturation resulted in less salivary leakage than gutta-percha with sealer when filling single root canals (24). Recently, OrthoMTA (BioMTA, Seoul, Korea) has been specifically developed for root canal obturation and has less heavy metal content than ProRoot MTA (25). In an *Enterococcus faecalis*-infected dentin model, OrthoMTA demonstrated bacterial entombment by intratubular mineralization after root canal obturation (26) and had minimal leakage compared to the

RealSeal SE obturation system using a glucose leakage model (27).

Various *in vitro* testing methods have been used to assess root canal filling quality including leakage tests using dye penetration or bacteria/endotoxin, sectioning and microscopic examination, and clearing techniques (24, 28-30). The shortcomings of these methods, however, include tooth destruction, lack of reproducibility, and the semi-quantitative nature of the data (30-32). The sectioning method also resulted in the formation of artifacts due to mechanical damage, and only a small number of useful slices were created per given root (32). Micro-CT can provide cross-sectional images of the obturated canals without damaging the teeth, and enables the calculation of quantitative three-dimensional volumes for root canal fillings (33,34). These cross-sectional micro-CT images correlate well with histological sections (35).

Therefore, the purpose of this study was to compare the filling quality of MTA canal obturation with lateral compaction and continuous wave of condensation in mesial root canals with type III canal configuration and the isthmus of the mandibular first molars using micro-CT. The null hypothesis was that there is no significant difference in filling quality among the three techniques in the main canal or isthmus.

II. Materials and Methods

A flow chart of this study is depicted in Figure 1.

Sample selection and root canal preparation

This study was approved by the Institutional Review Board of Seoul National University Dental Hospital (CRI 12006). Extracted human mandibular first molars were collected and stored in 10% neutral buffered formalin. 60 teeth were selected that had mesial roots with two separate canals extending from the pulp chamber to the apex, type III canal configuration by Weine (36), as confirmed by periapical radiographs.

Access opening was performed with a #4 round bur and Endo Z bur (Dentsply Maillefer, Ballaigues, Switzerland). #2 Gates Glidden burs (Dentsply Maillefer) were used for coronal flaring. Working length was established by inserting a #10 K-file (Dentsply Maillefer) into the mesiobuccal and mesiolingual canals until the tip of the file was just visible at the apical foramen with a dental operating microscope (OPMI Pico, Carl Zeiss Surgical GmbH, Oberkochen, Germany). Prior to instrumentation, canal curvature was viewed on radiographs taken from both buccal and mesial directions with #15 K-files (Dentsply Maillefer) inserted into the mesiobuccal and mesiolingual canals (37). Their curvatures (radius and degree) were measured with paint.NET

software version 3.5 (dotPDN LLC, Kirkland, WA, USA).

The mesial root canals were cleaned and shaped with ProTaper Next Ni-Ti rotary files (Dentsply Maillefer) according to the manufacturer's instructions until the X4 file (apical size #40) reached working length. Between each instrumentation step, the canals were irrigated with 1 ml of 3.5% sodium hypochlorite (NaOCl) solution delivered in a syringe with a 30-gauge needle (Max-i-Probe needle; Dentsply Rinn, Elgin, IL, USA). After instrumentation was completed, each canal was rinsed with 10 ml of 17% ethylenediaminetetraacetic acid (EDTA) to remove the smear layer, and then flushed with 10 ml of 3.5% NaOCl (38). Finally, the canals were cleaned ultrasonically with 3.5% NaOCl by the PerioScan ultrasonic unit with an Endospitze No. 5 irrigation tip (#20) (Sirona Dental Systems, Bensheim, Germany). The ultrasonic tip was placed as far apically inside the canal as it would go without binding, and then moved up and down 2-3 mm for 30s at low power, according to the manufacturer's instructions.

Root canal obturation

The prepared roots were allocated into three groups for obturation by the three different techniques so that there was an equitable distribution of canal curvature (radius and degree) between groups, as confirmed by one-way ANOVA (Table 1).

The root canal filling materials used in this study are described in Table 2.

LC group (n=20)

A standardized #40 master cone (Diadent, Chungju, Korea) was coated with AH Plus sealer (Dentsply, Johnson City, TN, USA) and placed to working length. A Ni-Ti Hyflex finger spreader size FM (Coltene/Whaledent, Mahwah, NJ, USA) was inserted to within 1-2 mm of the working length and removed (39). A sealer-coated FM accessory cone (Meta Biomed, Chungju, Korea) was placed. Three to five accessory cones were inserted until the spreader could not penetrate more than 3 mm into the canal orifice.

CW group (n=20)

The continuous wave of condensation technique was performed as described by Buchanan (10). A #40/.06 gutta-percha cone (Diadent) was fitted and trimmed to obtain a tug back 1 mm short of the working length, and then coated with AH Plus sealer. A B&L-alpha II tip (B&L Biotech, Ansan, Korea) was heated to 200°C and inserted into the master cone until it was 4-5 mm from the working length. Apical pressure was maintained without heat until the gutta-percha cooled. Then, heat was reapplied to the B&L-alpha II tip for one second as it was retrieved, and the remaining gutta-percha was compacted

with a cold S-Kondenser (Obtura Spartan, Fenton, MO, USA). The coronal portion of the canal was obturated with B&L-Beta (B&L Biotech) using a regular type GP pellet (B&L Biotech), and vertically condensed with S-Kondenser.

MTA group (n=20)

MTA canal obturation was performed with OrthoMTA (26). OrthoMTA was used to fill the root canals following the manufacturer's guidelines (40). The cap of the vial holding OrthoMTA powder was opened and distilled water was added. OrthoMTA powder was mixed with a sterilized stick. The vial was centrifuged for 20s using the OrthoMTA automixer (BioMTA), and any excess water was removed with a cotton swab. OrthoMTA paste was packed into the OrthoMTA carrier (BioMTA) with a gentle tapping motion, and introduced into the canal. A sterile OrthoMTA compactor (BioMTA; size #25/.02) was used. The compactor was inserted to working length and applied with a circumferential filing motion at 60 rpm. After obtaining an apical stop, the S-Kondensor was used to compact the material.

All of the canal preparations and obturation procedures were performed by one endodontist to ensure consistency. Following obturation, the teeth were stored at 37°C with 100% humidity for seven days to allow for the complete setting of the sealer (LC,

CW) and OrthoMTA.

Micro-CT scanning and image reconstruction

The obturated mesial roots were scanned by high-resolution micro-CT (Skyscan 1172; Bruker-Micro-CT, Kontich, Belgium) at 100 kV and 100 μA using 0.5 mm-thick aluminum filter and 30% beam hardening reduction, which had a rotational step of 0.5° and a cross-sectional pixel size of 14.87 μm. From these scans, cross-sectional images were reconstructed with NRecon software (version 1.6.9.18; Bruker-Micro-CT) to show two-dimensional slices of the internal root canal anatomy. The CTAn software (version 1.11.0.0; Bruker-Micro-CT) was further employed for volumetric analysis and quantification of the filling materials and voids. Three-dimensional (3D) models were created for visualization of the obturated root canals with CTVol software (version 2.1.1.2; Bruker-Micro-CT) and Dataviewer (version 1.4.2.2; Bruker-Micro-CT).

After micro-CT scanning, three specimens in each group were sectioned horizontally using a low-speed diamond disk (NTI, Kahla, Germany) 1, 2, 3, and 4 mm from the apex under water cooling. Differentiating the different substrates was based on the difference of gray scale index. The gray scale index ranged from 0 to 255 according to the density of the substrate. The regions of gutta-percha, sealer, or MTA were determined by choosing

the range of gray scale values (Figs. 2 & 3). Isthmus selection was carried out using a criterion of a mesio-distal width less than one-third of the diameter of the main canal (Fig. 4).

The frequency of complete and incomplete isthmuses and the mean total isthmus volume in the apical 5 mm were compared between groups using the Kruskal-Wallis test.

Micro-CT was used to quantify the canal volume, the filled volume, and the volume of the voids distributed along the canal walls (interface void volume). The filled volume was defined as the sum of the gutta-percha and sealer occupied volume in the LC and CW obturated canals, and the volume of the filled OrthoMTA in the MTA group. The filled volume ratios and the gutta-percha and sealer volume ratios were calculated as a percentage of the main canal or isthmus volume for the apical 5 mm of the canals. The Kruskal-Wallis test was used to compare the filled volume ratios and interface void volume ratios among the three groups in the main canals, and the filled volume ratio in the isthmus. The Mann-Whitney U test was used to compare the gutta-percha and sealer volume ratio between the LC and CW groups. IBM SPSS version 21 software package (IBM Corp, Armonk, NY, USA) was used, and the level of significance was set at $p < 0.05$.

To evaluate the distribution of the filling materials in the

isthmus, the ratio of filling materials to isthmus area of each axial slice was calculated. The axial-slice was examined at 0.1-mm intervals from 0.5 to 5.0 mm from the apical end of the working length in each root by CTAn software. The ratio of filling materials to isthmus area was further identified as the ratio of gutta-percha or sealer occupied area to isthmus area in groups LC and CW.

III. Results

Three-dimensional reconstructed images of the obturated root canals are shown in Figures 5 and 6. Unfilled isthmus was observed in all of the obturation groups. Representative 3D visualizations of the gutta-percha, sealer, OrthoMTA, and voids in each group are shown in Figures 7-9. Root canal sealer was evenly distributed throughout the lengths of the roots in group LC (Fig. 7). Partially-filled isthmus with gutta-percha was identified in the roots of the CW group (Fig. 8).

There were no significant differences between the groups in the frequency of complete and incomplete isthmuses, and in the mean total isthmus volume ($p > 0.05$) (Table 3). In the main canals, there were no significant differences in the filled volume ratios or gutta-percha and sealer volume ratios between the LC

and CW groups ($p > 0.05$) (Table 4). However, the LC group showed a significantly higher interface void volume ratio than CW or MTA ($p < 0.05$).

With regard to the isthmus, the filled volume ratio in the LC group was significantly lower than in the CW or MTA groups ($p < 0.05$). The gutta-percha volume ratio was also significantly lower in the LC group than in the CW group ($p < 0.05$). However, the sealer volume ratio was significantly higher in the LC group than that in the CW group ($p < 0.05$).

The ratios of filling materials to isthmus area in the axial slice images were plotted along the apical 5 mm of the working length (Fig. 10). The greatest percentage of filling materials was found at 0.5-0.6 and 4.6-4.7 mm from the apical end of the working length for the LC group, whereas the greatest percentage was found 1.3-2.1 and 4.0-5.0 mm from the apical end of the working length in the CW group. The greatest ratio of gutta-percha in the isthmus area was at the 4-5 mm level, and this gradually decreased towards the apex in both groups LC and CW. The ratio of filled MTA to isthmus area was greatest at 0.5-1 mm from the working length, and remained relatively high until 3.5 mm from the apex as compared to LC or CW.

Figure 11 shows the coronal, axial, and sagittal micro-CT images of the MTA group and LC groups, and shows the unfilled

radiolucent voids.

Ⅳ. Discussion

This study used high-resolution micro-CT to evaluate the filling quality of MTA canal obturation in type III mesial root canals of the mandibular first molars. The apical 5 mm region was analyzed as this area has been reported to have the highest prevalence of isthmus (3, 41). The micro-CT was an effective tool in distinguishing between filling materials such as gutta-percha, sealer, or MTA from the surrounding root canal dentin walls and void spaces, as shown in prior studies (33-35).

The present results showed that the main canals obturated by LC had a significantly higher interface void volume ratio than those obturated by CW or MTA. There were straight linear voids at the interface between the gutta-percha and dentin in the LC group. These voids might result from the spreader tracts during lateral compaction, which have been reported in a previous study (42), and can become passageway for bacterial leakage and eventual endodontic failure (43).

The incomplete filling of the isthmus observed in the micro-CT images might be due to the presence of pulp tissue remnants and prepared dentin debris. A previous micro-CT study found

dentin debris packed into the isthmus of the mesial roots of the mandibular molars (44). The authors reported that there was much less filling of the isthmus volume (57.5%) compared to the main canals (98.5%) (44). Another micro-CT study demonstrated that one third of the isthmus volume contained hard tissue debris when the mesial root canals of the mandibular molars were prepared without irrigation (45).

Even when filling materials adequately fill the root canals, gutta-percha does not chemically bond to dentin, whereas MTA can form a mineralized layer at the interface of dentin and MTA (18, 26, 27, 46). This layer with tag-like structures contains calcium and phosphorus, which optimize the sealing ability of the MTA-filled root canals, and thus results in bacterial entombment in the dentinal tubules of experimentally-infected root canals (26).

The micro-CT images shown as uneven densities in the MTA group (Figs. 5 & 6) may have been due to variations in the mineral components or inherent porosities of the material during hydration. These macro- and micro- porosities could be caused by an inadequate water-to-powder ratio, insufficient packing, or water evaporation (19, 20, 34). MTA canal obturation in curved canals is technique-sensitive. Unfilled voids were formed in a few samples in the MTA group because mixed MTA paste did not fill the linear space after the use of the OrthoMTA compactor.

Several specimens in the MTA group showed overfilling, which might be due to the use of the compactor at working length, which was according to the manufacturer's guidelines. Although a previous case report clearly demonstrated that periapical radiolucent lesions around an extruded MTA was resolved in the follow-up radiographs of teeth with open apices (48), the validity of the overfilling results needs further investigation through *in vitro* or *in vivo* studies.

Although it has been reported that the voids or pores caused by dissolution of calcium hydroxide within MTA could be 'self-repaired' by mineral precipitates such as a calcium silicate hydrate gel formed by the hydration reaction of the material (47, 48), there are concerns regarding the possibility of bacteria ingress by the formation of internal voids within the MTA after obturation (34). Therefore, MTA canal obturation should be carefully performed to minimize the possible formation of voids and pores, and should be limited to selected cases until its long-term benefits and prognosis can be confirmed.

Ⅴ. Conclusions

The filled volume ratio of MTA canal obturation was comparable to root canal obturation techniques using gutta-

percha with sealer in the main canal and isthmus.

VI. References

1. Schilder H. Filling root canals in three dimensions. Dent Clin North Am. 1967:723-44.

2. American Association of Endodontists. Glossary of endodontic terms. Chicago, IL: American Association of Endodontists; 2012.

3. Mannocci F, Peru M, Sherriff M, Cook R, Pitt Ford TR. The isthmuses of the mesial root of mandibular molars: a micro-computed tomographic study. Int Endod J. 2005;38(8):558-63.

4. Fan B, Pan Y, Gao Y, Fang F, Wu Q, Gutmann JL. Three-dimensional morphologic analysis of isthmuses in the mesial roots of mandibular molars. J Endod. 2010;36(11):1866-9.

5. Nair PN, Henry S, Cano V, Vera J. Microbial status of apical root canal system of human mandibular first molars with primary apical periodontitis after "one-visit" endodontic treatment. Oral Surg Oral Med Oral Pathol Oral Radiol Endod. 2005;99(2):231-52.

6. von Arx T. Frequency and type of canal isthmuses in first molars detected by endoscopic inspection during periradicular surgery. Int Endod J. 2005;38(3):160-8.

7. Carr GB, Schwartz RS, Schaudinn C, Gorur A, Costerton JW. Ultrastructural examination of failed molar retreatment with secondary apical periodontitis: an examination of endodontic biofilms in an endodontic retreatment failure. J Endod. 2009;35(9):1303-9.

8. Clinton K, Van Himel T. Comparison of a warm gutta-percha obturation technique and lateral condensation. J Endod. 2001;27(11):692-5.

9. Keleş A, Ahmetoglu F, Uzun I. Quality of different gutta-percha

techniques when filling experimental internal resorptive cavities: a micro-computed tomography study. Aust Endod J. 2014;40(3):131-5.

10. Buchanan LS. The continuous wave of condensation technique: a convergence of conceptual and procedural advances in obturation. Dent Today. 1994;13(10):80, 2, 4-5.

11. Lee FS, Van Cura JE, BeGole E. A comparison of root surface temperatures using different obturation heat sources. J Endod. 1998;24(9):617-20.

12. Lipski M. Root surface temperature rises during root canal obturation, in vitro, by the continuous wave of condensation technique using System B HeatSource. Oral Surg Oral Med Oral Pathol Oral Radiol Endod. 2005;99(4):505-10.

13. Molyvdas I, Zervas P, Lambrianidis T, Veis A. Periodontal tissue reactions following root canal obturation with an injection-thermoplasticized gutta-percha technique. Endod Dent Traumatol. 1989;5(1):32-7.

14. Ørstavik D, Nordahl I, Tibballs JE. Dimensional change following setting of root canal sealer materials. Dent Mater. 2001;17(6):512-9.

15. Zhou HM, Shen Y, Zheng W, Li L, Zheng YF, Haapasalo M. Physical properties of 5 root canal sealers. J Endod. 2013;39(10):1281-6.

16. Parirokh M, Torabinejad M. Mineral trioxide aggregate: a comprehensive literature review--Part I: chemical, physical, and antibacterial properties. J Endod. 2010;36(1):16-27.

17. Torabinejad M, Watson TF, Pitt Ford TR. Sealing ability of a mineral trioxide aggregate when used as a root end filling material. J Endod. 1993;19(12):591-5.

18. Sarkar NK, Caicedo R, Ritwik P, Moiseyeva R, Kawashima I. Physicochemical basis of the biologic properties of mineral trioxide aggregate. J Endod. 2005;31(2):97-100.

19. Saghiri MA, Asgar K, Lotfi M, Karamifar K, Neelakantan P, Ricci JL. Application of mercury intrusion porosimetry for studying the porosity of mineral trioxide aggregate at two different pH. Acta Odontol Scand. 2012;70(1):78-82.

20. Fridland M, Rosado R. Mineral trioxide aggregate (MTA) solubility and porosity with different water-to-powder ratios. J Endod. 2003;29(12):814-7.

21. Boutsioukis C, Noula G, Lambrianidis T. Ex vivo study of the efficiency of two techniques for the removal of mineral trioxide aggregate used as a root canal filling material. J Endod. 2008;34(10):1239-42.

22. Felman D, Parashos P. Coronal tooth discoloration and white mineral trioxide aggregate. J Endod. 2013;39(4):484-7.

23. Bogen G, Kuttler S. Mineral trioxide aggregate obturation: a review and case series. J Endod. 2009;35(6):777-90.

24. Al-Hezaimi K, Naghshbandi J, Oglesby S, Simon JH, Rotstein I. Human saliva penetration of root canals obturated with two types of mineral trioxide aggregate cements. J Endod. 2005;31(6):453-6.

25. Chang SW, Baek SH, Yang HC, Seo DG, Hong ST, Han SH, Lee Y, Gu Y, Kwon HB, Lee W, Bae KS, Kum KY. Heavy metal analysis of ortho MTA and ProRoot MTA. J Endod. 2011;37(12):1673-6.

26. Yoo JS, Chang SW, Oh SR, Perinpanayagam H, Lim SM, Yoo YJ, Oh YR, Woo SB, Han SH, Zhu Q, Kum KY. Bacterial entombment by intratubular mineralization following orthograde mineral trioxide

aggregate obturation: a scanning electron microscopy study. Int J Oral Sci. 2014;6(4):227-32.

27. Kim SY, Kim KJ, Yi YA, Seo DG. Quantitative microleakage analysis of root canal filling materials in single-rooted canals. Scanning. 2015;37(4):237-45.

28. Schäfer E, Nelius B, Burklein S. A comparative evaluation of gutta-percha filled areas in curved root canals obturated with different techniques. Clin Oral Investig. 2012;16(1):225-30.

29. Barbosa FO, Gusman H, Pimenta de Araújo MC. A comparative study on the frequency, location, and direction of accessory canals filled with the hydraulic vertical condensation and continuous wave of condensation techniques. J Endod. 2009;35(3):397-400.

30. Wu MK, Wesselink PR. Endodontic leakage studies reconsidered. Part I. Methodology, application and relevance. Int Endod J. 1993;26(1):37-43.

31. van der Borden WG, Wu MK, Wesselink PR. Percentages of gutta-percha-filled canal area observed after increased apical enlargement. J Endod. 2010;36(1):139-42.

32. Marciano MA, Ordinola-Zapata R, Cunha TV, Duarte MA, Cavenago BC, Garcia RB, Bramante CM, Bernardineli N, Moraes IG. Analysis of four gutta-percha techniques used to fill mesial root canals of mandibular molars. Int Endod J. 2011;44(4):321-9.

33. Hammad M, Qualtrough A, Silikas N. Evaluation of root canal obturation: a three-dimensional in vitro study. J Endod. 2009;35(4):541-4.

34. El-Ma'aita AM, Qualtrough AJ, Watts DC. A micro-computed tomography evaluation of mineral trioxide aggregate root canal

fillings. J Endod. 2012;38(5):670-2.

35. Jung M, Lommel D, Klimek J. The imaging of root canal obturation using micro-CT. Int Endod J. 2005;38(9):617-26.

36. Weine FS. Endodontic Therapy. 5th ed. St. Louis1996.

37. Schäfer E, Diez C, Hoppe W, Tepel J. Roentgenographic investigation of frequency and degree of canal curvatures in human permanent teeth. J Endod. 2002;28(3):211-6.

38. Yamada RS, Armas A, Goldman M, Lin PS. A scanning electron microscopic comparison of a high volume final flush with several irrigating solutions: Part 3. J Endod. 1983;9(4):137-42.

39. Allison DA, Michelich RJ, Walton RE. The influence of master cone adaptation on the quality of the apical seal. J Endod. 1981;7(2):61-5.

40. BioMTA. OrthoMTA Seoul, Republic of Korea [accessed 2015 April 09]. Available from: http://www.biomta.com/shop/eng/product_1.php

41. Jung IY, Seo MA, Fouad AF, Spångberg LS, Lee SJ, Kim HJ, Kum KY. Apical anatomy in mesial and mesiobuccal roots of permanent first molars. J Endod. 2005;31(5):364-8.

42. Keleş A, Alcin H, Kamalak A, Versiani MA. Micro-CT evaluation of root filling quality in oval-shaped canals. Int Endod J. 2014;47(12):1177-84.

43. Nair PN. On the causes of persistent apical periodontitis: a review. Int Endod J. 2006;39(4):249-81.

44. Endal U, Shen Y, Knut A, Gao Y, Haapasalo M. A high-resolution computed tomographic study of changes in root canal isthmus area by instrumentation and root filling. J Endod. 2011;37(2):223-7.

45. De-Deus G, Marins J, Neves Ade A, Reis C, Fidel S, Versiani MA, Alves H, Lopes RT, Paciornik S. Assessing accumulated hard-tissue debris using micro-computed tomography and free software for image processing and analysis. J Endod. 2014;40(2):271-6.

46. Reyes-Carmona JF, Felippe MS, Felippe WT. Biomineralization ability and interaction of mineral trioxide aggregate and white portland cement with dentin in a phosphate-containing fluid. J Endod. 2009;35(5):731-6.

47. Camilleri J. Hydration mechanisms of mineral trioxide aggregate. Int Endod J. 2007;40(6):462-70.

48. Han L, Okiji T, Okawa S. Morphological and chemical analysis of different precipitates on mineral trioxide aggregate immersed in different fluids. Dent Mater J. 2010;29(5):512-7.

Table 1. Buccal and proximal views of the angle and radius of the curved mesial root canals of the three groups

Buccal view

Group	Curvature (degrees)			Radius (mm)		
	Mean	SD	Range	Mean	SD	Range
LC	16.42	4.39	10.70-25.90	6.99	1.63	4.45-9.12
CW	16.41	3.84	10.60-25.70	7.24	1.62	5.02-9.35
MTA	17.02	3.81	10.87-24.70	7.31	1.65	4.68-9.68
	$p = 0.745$			$p = 0.156$		

Proximal view

Group	Curvature (degrees)			Radius (mm)		
	Mean	SD	Range	Mean	SD	Range
LC	14.22	3.36	10.10-32.00	7.26	1.93	4.04-9.98
CW	14.13	2.98	10.20-29.10	7.27	2.11	4.01-10.10
MTA	14.57	3.43	10.70-28.60	7.48	2.08	4.09-9.95
	$p = 0.877$			$p = 0.694$		

Table 2. Manufacturer and composition of root filling materials used in this study

Filling materials	Manufacturer	Composition
Standardized master cone #40/.06 master cone	Diadent	Gutta-percha polymer, wax/resins, zinc oxide, barium sulfate, coloring agents, antioxidants
Accessory cone	Meta Biomed	
AH Plus sealer	Dentsply	Paste A: Biophenol-A epoxy resin, Bisphenol-F epoxy resin, calcium tungstate, zirconium oxide, silica, iron oxide pigments Paste B: Dibenzyldiamine, aminoadamantane, tricyclodecane-diamine, calcium tungstate, zirconium oxide, silica, silicone oil
OrthoMTA	BioMTA	tricalcium silicate, dicalcium silicate, tricalcium aluminate, bismuth oxide, calcium carbonate

Table 3. Types of isthmuses and their total volume (mean ± SD) allocated into three groups

Type of Isthmus		LC	CW	MTA	Statistical differences
Incomplete	number	10	10	10	NS
Isthmus	Volume (mm^3)	0.0691 ± 0.0392	0.0652 ± 0.0332	0.0645 ± 0.0312	NS
Complete	number	10	10	10	NS
Isthmus	Volume (mm^3)	0.3098 ± 0.4531	0.3129 ± 0.2447	0.3227 ± 0.2662	NS

NS: not significant

Volume: sum of filled and unfilled volumes in each isthmus

Table 4. Filled and void volumes in the main canals and isthmuses in the apical 5 mm of the obturated canals

Volume (%)		Group		
		LC	**CW**	**MTA**
Main canal	Filled volume	99.22±0.21[a]	99.72±0.13[a]	99.79±0.38[a]
	Gutta-percha volume	91.70±4.75[a]	93.13±4.29[a]	N/A
	Sealer volume	8.04±4.76[a]	6.55±4.27[a]	N/A
	Interface void volume	0.77±0.16[b]	0.27±0.12[a]	0.19±0.19[a]
Isthmus	Filled volume	61.15±12.46[a]	80.11±12.99[b]	82.98±9.75[b]
	Gutta-percha volume	43.26±14.32[a]	71.03±12.68[b]	N/A
	Sealer volume	17.88±12.05[b]	9.07±6.03[a]	N/A

N/A: not applicable.

The same superscript lowercase letter in each row indicates no significant differences between obturation techniques ($p > 0.05$).

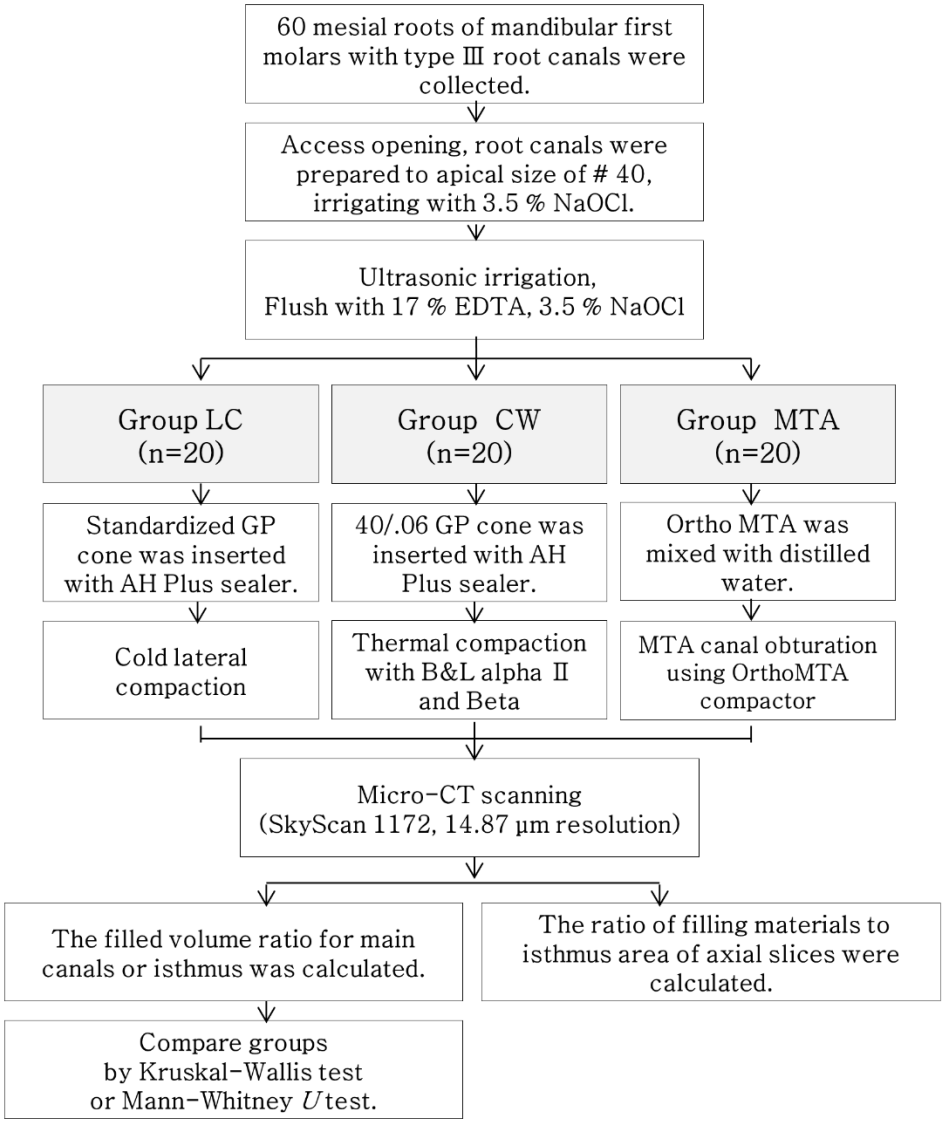

Figure 1. A flow chart of this study

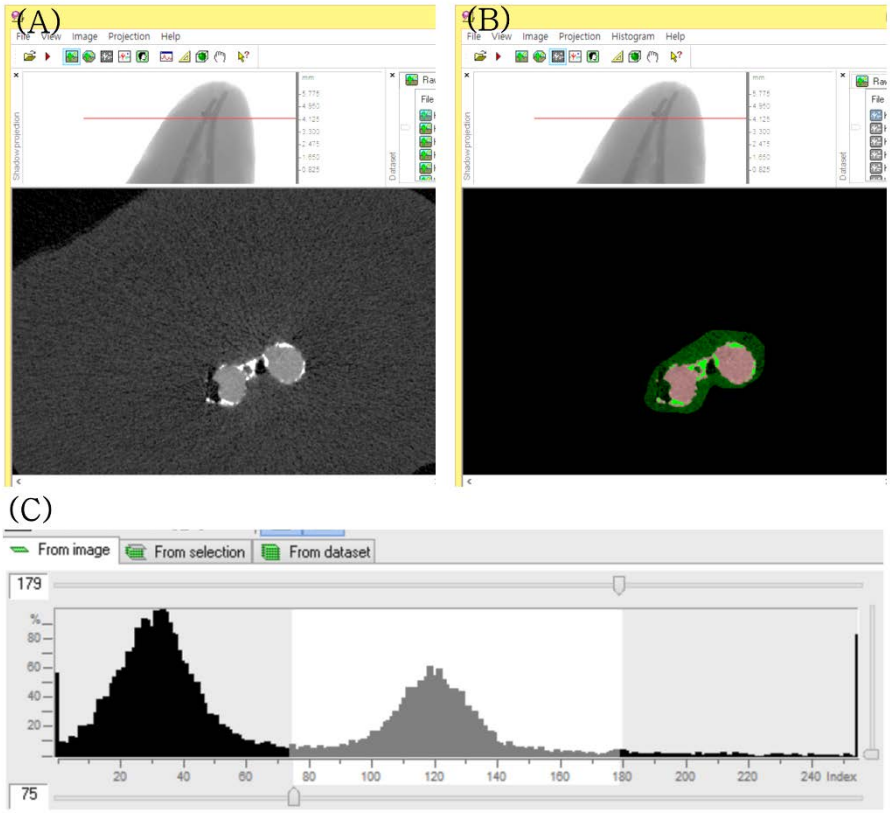

Figure 2. Determination of the area for gutta-percha and sealer in the micro-CT image

(A) Original cross-sectional image; (B) Areas of gutta-percha, sealer, and voids were shown in red, light, and black, respectively; (C) Gray scale range (75-179) corresponding to gutta-percha was selected.

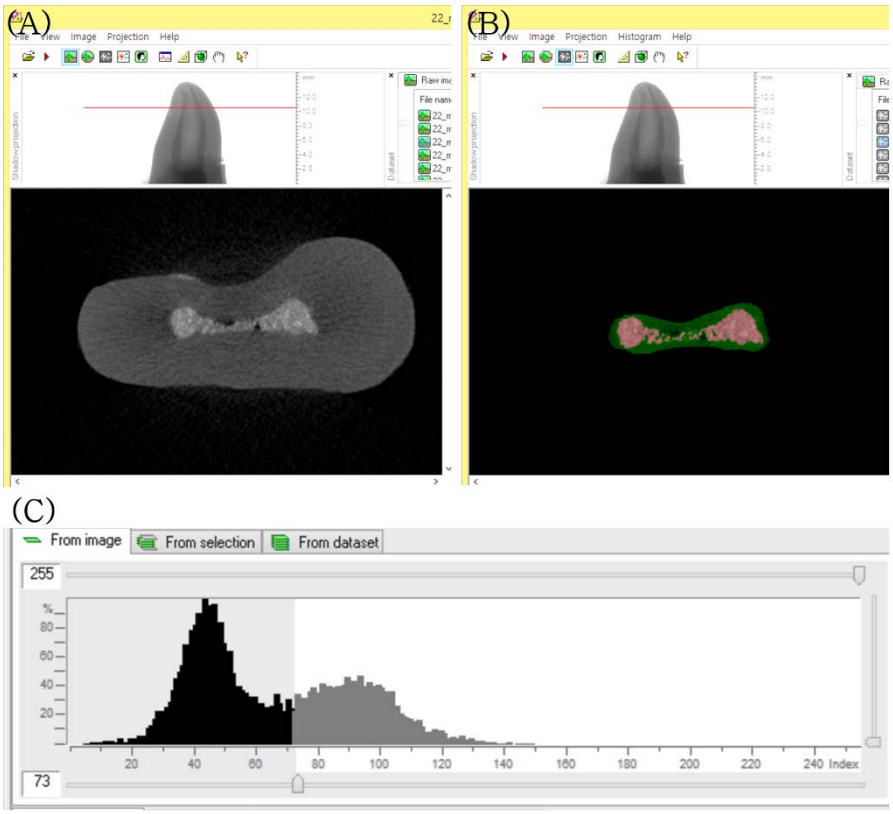

Figure 3. Determination of area for OrthoMTA in the micro-CT image (A) Original cross-sectional image; (B) Areas of OrthoMTA and voids were shown in red and black, respectively; (C) Gray scale range (73-255) corresponding to OrthoMTA was selected.

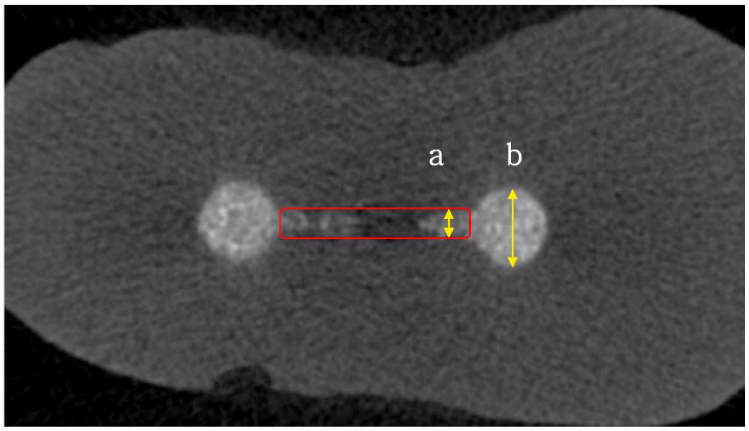

Figure 4. Determination of isthmus area in a cross-sectional micro-CT image.

(a) Mesio-distal width of isthmus; (b) Diameter of main canal; Isthmus area was determined (red rectangle) as (a) is less than one-third of (b).

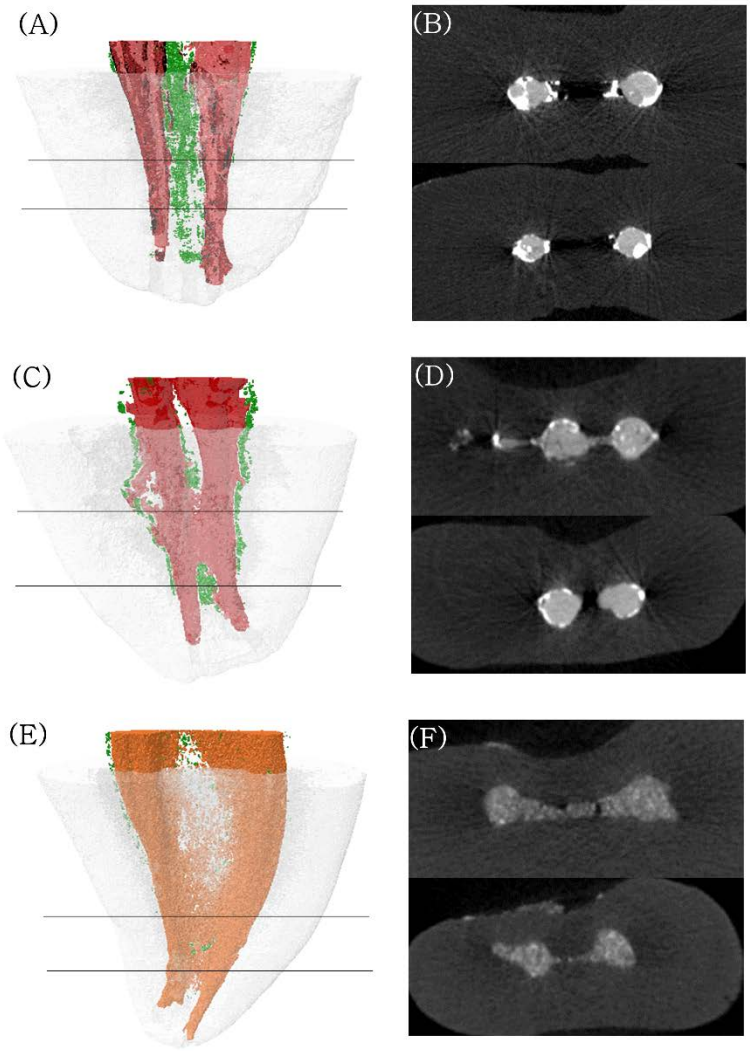

Figure 5. 3D-reconstructed images of the obturated mesial root canals of the mandibular first molars with complete isthmuses.
(A, B) group LC; (C, D) group CW; (E, F) group MTA.
(A, C, E) gutta-percha (red), sealer (black), MTA (orange), and unfilled canal space (green); (B, D, F) Cross-sectional images at the level of the solid lines (black) of (A, C, E), (magnification ×8). (B) 2.0, 3.2 mm; (D) 1.7, 3.3 mm; (F) 1.2, 2.9 mm levels from the apical end of working length.

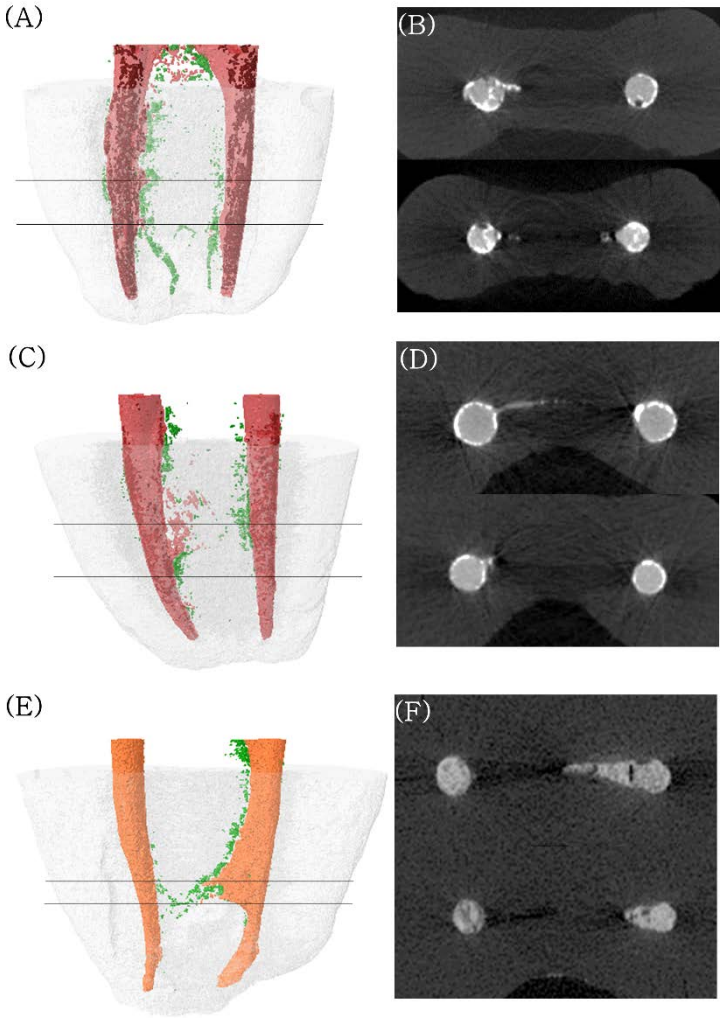

Figure 6. 3D-reconstructed images of the obturated mesial root canals of the mandibular first molars with incomplete isthmuses. (A, B) group LC; (C, D) group CW; (E, F) group MTA.
(A, C, E) gutta-percha (red), sealer (black), MTA (orange), and unfilled canal space (green); (B, D, F) Cross-sectional images at the level of the solid lines (black) of (A, C, E), (magnification ×8). (B) 2.0, 3.4 mm; (D) 2.1, 3.8 mm; (F) 1.6, 4.8 mm levels from the apical end of working length.

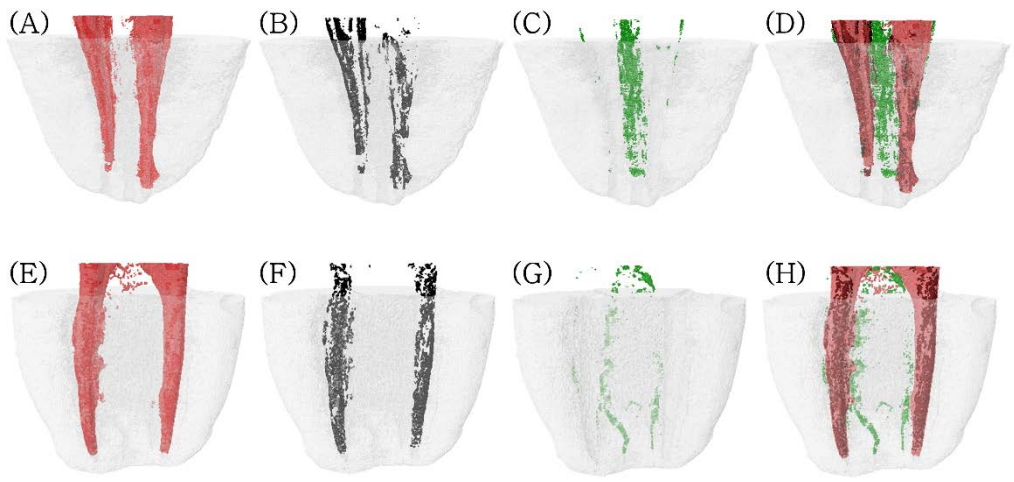

Figure 7. 3D visualization of the root canals of the LC group. (A-D): root canals with complete isthmuses; Depiction of the filled gutta-percha (A), sealer (B), voids in the root canal system (C), composite images of root canal fillings and voids (D); (E-H): root canals with incomplete isthmuses; Depiction of the filled gutta-percha (E), sealer (F), voids in the root canal system (G), composite images of the root canal fillings and voids (H).

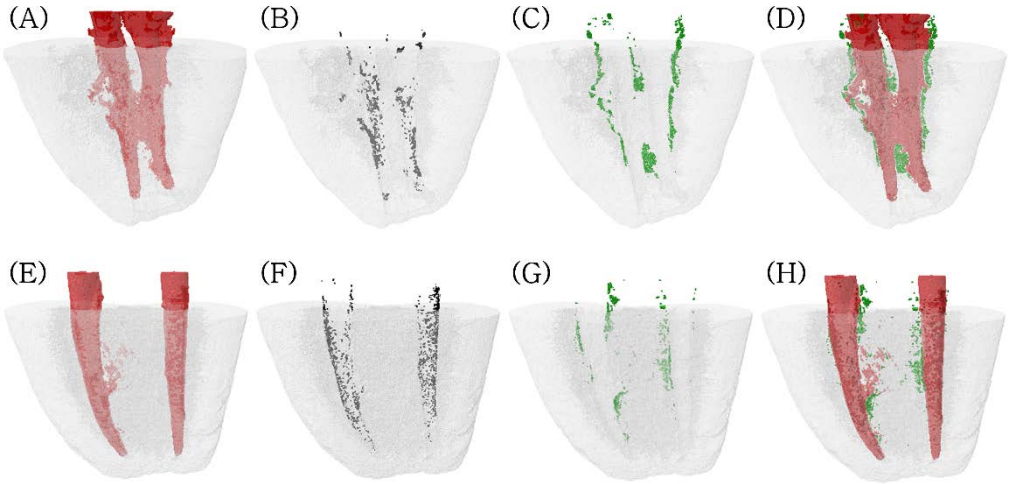

Figure 8. 3D visualization of the root canals of the CW group. (A-D): root canals with complete isthmuses; Depiction of the filled gutta-percha (A), sealer (B), voids in the root canal system (C), composite images of root canal fillings and voids (D); (E-H): root canals with incomplete isthmuses; Depiction of the filled gutta-percha (E), sealer (F), voids in the root canal system (G), composite images of root canal fillings and voids (H).

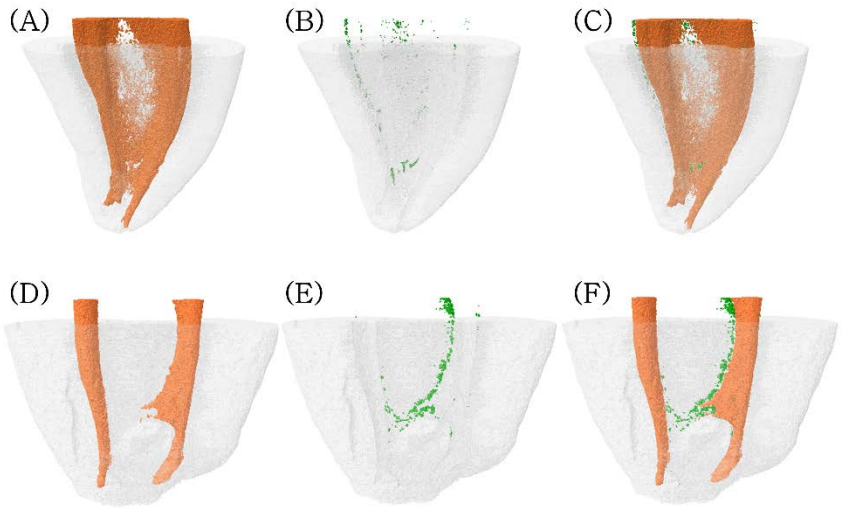

Figure 9. 3D visualization of the root canals of the MTA group. (A-C): root canals with complete isthmuses; Depiction of the filled OrthoMTA (A), voids within the root canal system (B), composite images of root canal fillings and voids (C); (D-F): root canals with incomplete isthmuses; Depiction of the filled OrthoMTA (D), voids in the root canal system (E), composite images of root canal fillings and voids (F).

(A)

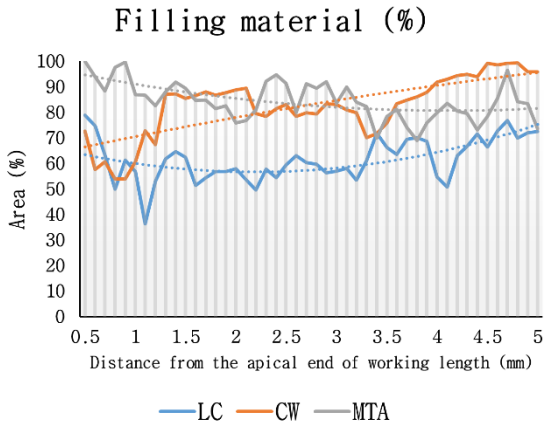
Filling material (%)
Area (%)
100
90
80
70
60
50
40
30
20
10
0
0.5
1
1.5
2
2.5
3
3.5
4
4.5
5
Distance from the apical end of working length (mm)
LC
CW
MTA

(B)

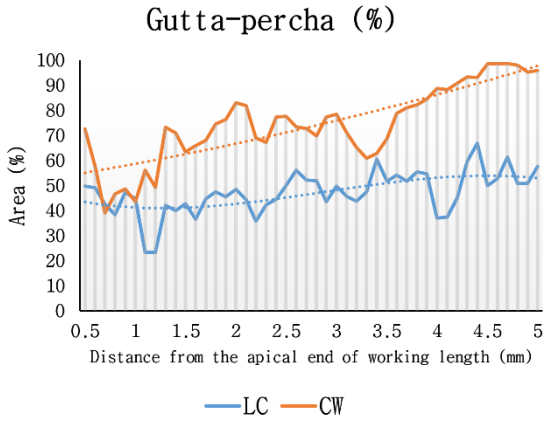
Gutta-percha (%)
Area (%)
100
90
80
70
60
50
40
30
20
10
0
0.5
1
1.5
2
2.5
3
3.5
4
4.5
5
Distance from the apical end of working length (mm)
LC
CW

(C)

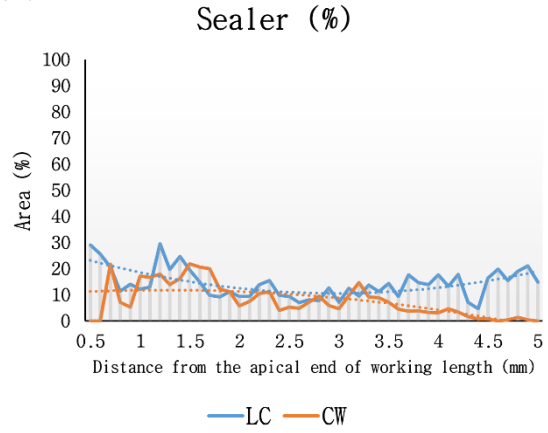
Sealer (%)
Area (%)
100
90
80
70
60
50
40
30
20
10
0
0.5
1
1.5
2
2.5
3
3.5
4
4.5
5
Distance from the apical end of working length (mm)
LC
CW

Figure 10. The percentage distribution of 2D filling materials in the isthmuses obturated using the LC, CW, or MTA techniques Surface area (%) (solid lines) occupied by (A) filling materials; (B) gutta-percha; (C) sealer, and their trends (dotted lines) for the three groups, at specified distances from the apical end of working length (mm). Filling materials were defined as the sum of the area of the filled gutta-percha and sealer in the LC and CW groups, and the filled area of OrthoMTA in the MTA group.

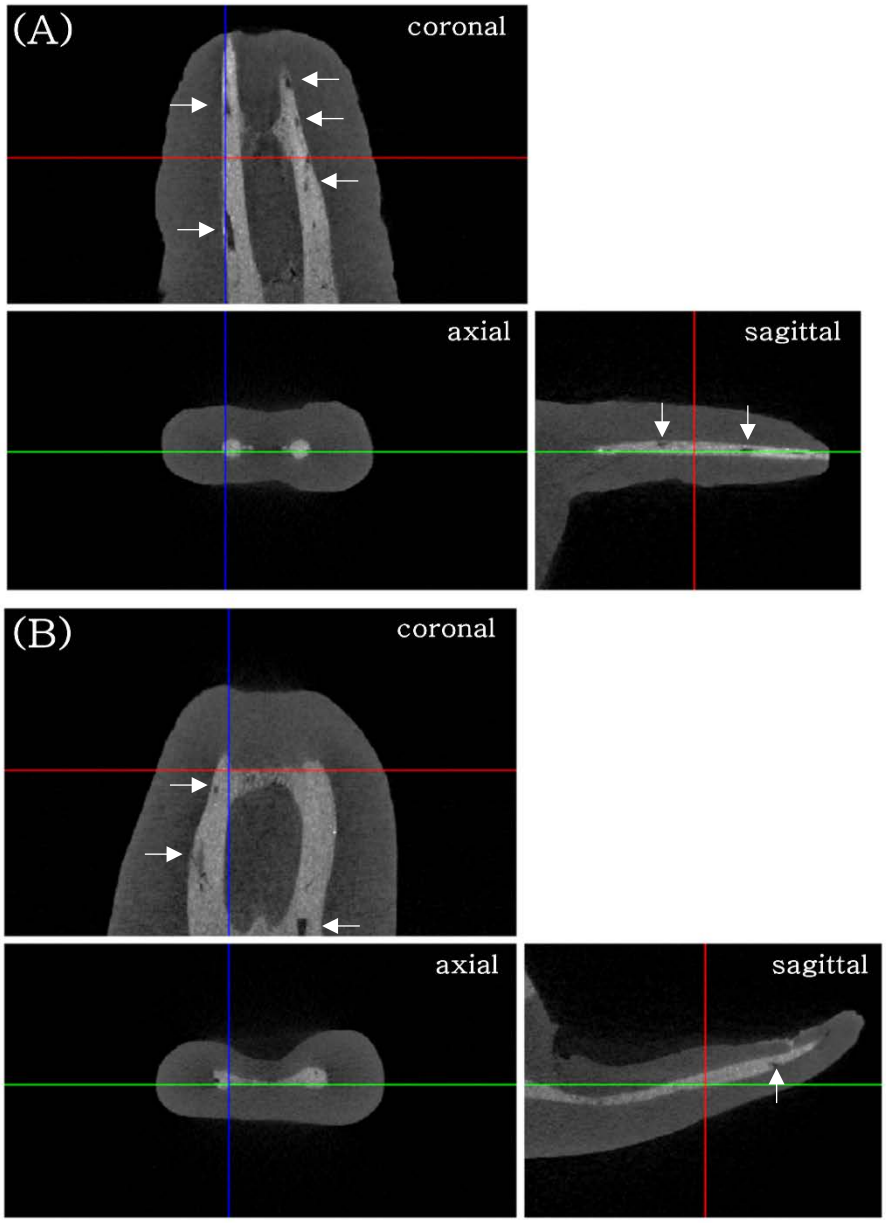
(A)
coronal
axial
sagittal
(B)
coronal
axial
sagittal

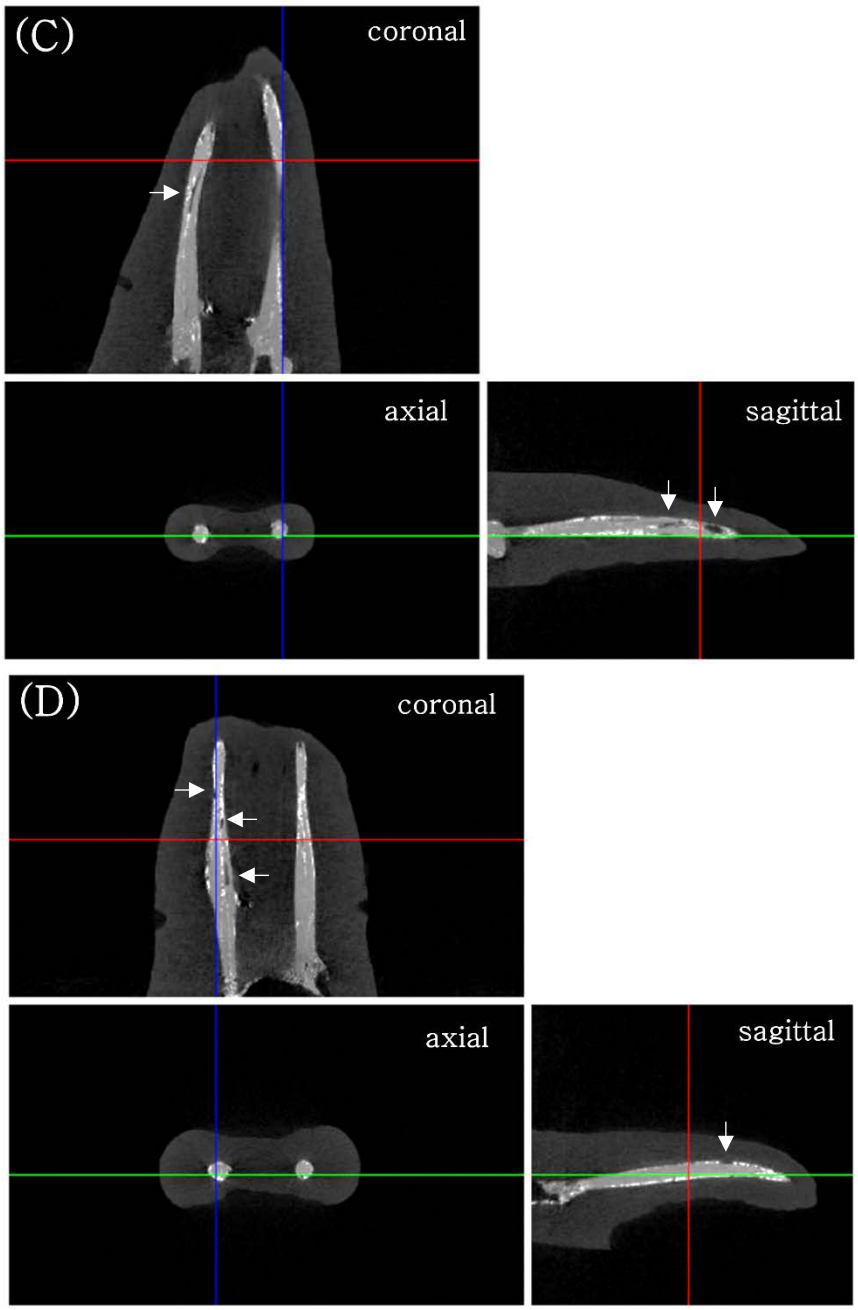

Figure 11. Two examples of reconstructed images possessing internal voids of the root canals of the MTA group (A, B) and the

LC group (C, D). Coronal, axial, and sagittal views are shown. Unfilled radiolucent voids are shown within the filled materials (arrows).

-국문초록-

Isthmus를 갖는 제 3형 근관에서 MTA를 이용한 근관 충전의 질적 평가

오 소 람

서울대학교 대학원 치의과학과 치과보존학 전공

(지도교수 금 기 연)

목적

이 연구의 목적은 isthmus를 갖는 제 3형 근관 형태인 하악 제1대구치 근심 근관에 MTA 근관 충전 (MTA 군)하여 측방 가압 충전법 (LC 군), continuous wave 가압법 (CW 군)과 미세 전산화 단층 촬영술을 이용하여 충전 질을 비교하는 것이다. 귀무가설은 주근관과 isthmus의 충전 질에 있어서 세 가지 충전 방법 간에 차이가 없다는 것이다.

재료 및 방법

Weine 분류법 제 3형의 근심 근관으로 두 개의 근심 근관

사이에 서로 연결되는 isthmus가 있는 하악 제1대구치 근심 치근 60개를 수집하여 근첨부 크기가 #40이 되도록 근관 형성하였다. 근관 형성한 근심 치근을 각 20개씩 3개의 군으로 나누어 다음과 같은 세 가지 방법으로 근관 충전하였다. 거타퍼차와 AH Plus 실러를 이용한 측방 가압 충전과 continuous wave 가압법을 이용하여 충전, 또는 OrthoMTA를 이용하여 MTA 근관 충전하였다.

충전한 치근을 미세 전산화 단층 촬영기기 (Skyscan 1172)를 이용하여 촬영하였다. CTAn 프로그램을 이용하여 근단부 삼분의 일 부위에서 주근관과 isthmus 내의 충전 부피비율을 계산하였다. 충전 부피비율은 LC 군과 CW 군에서는 주근관 또는 isthmus의 부피에 대한 충전된 거타퍼차와 실러의 부피의 합의 비율로, MTA 군에서는 충전된 MTA의 부피의 비율로 정의하였다. 충전 방법에 따른 충전 부피비율을 Kruskal-Wallis test와 Mann-Whitney U test를 이용하여 비교하였다.

결과

재구성된 미세 전산화 단층 사진에서 LC 군은 CW 군이나 MTA 군에 비해 isthmus에서 낮은 충전 밀도를 나타내었다. MTA 군의 2개 시편에서 충전되지 않은 방사선 투과상 공극이 관찰되었다. 주근관에서 충전 부피비율은 그룹 간 차이를 나타내지 않았다 ($p > 0.05$). LC 군의 isthmus 내 충전 부피비율은 CW 군과 MTA 군에 비해 낮았다 ($p < 0.05$). LC 군의 isthmus 내 거타퍼차의

부피비율은 CW 군에 비해 낮았으나 실러의 부피비율은 더 높았다 ($p < 0.05$).

결론

MTA 근관 충전은 측방 가압 충전법, continuous wave 가압법과 비교시 주근관과 isthmus에서 대등한 충전 부피비율을 나타내었다.

주요어: MTA 근관 충전, 충전 부피비율, isthmus, 미세 전산화 단층 촬영술, 하악 제1 대구치, 제 3형 근관

학 번: 2011-30664